Climate warming as a possible trigger of freshwater pearl mussel population decline in oligotrophic rivers throughout Europe

Yulia V. Bespalaya[1,2], Ivan N. Bolotov [1,2], Alexander A. Makhrov[3], Mikhail Yu. Gofarov[1,2], Olga V. Aksenova[1,2], Paul E. Aspholm[4], Mikhail B. Kabakov[1], Yulia S. Kolosova[1,2], Alexander V. Kondakov[1,2], Thomas Ofenböck[5], Andrew N. Ostrovsky[6,7], Igor Yu. Popov[8], Ted von Proschwitz [9], Mudīte Rudzīte[10], Māris Rudzītis[10], Svetlana E. Sokolova[1], Ilmari Valovirta[11], Ilya V. Vikhrev[1,2], Maxim V. Vinarski[12] & Alexey A. Zotin[13]

[1]N. Laverov Federal Center for Integrated Arctic Research, Russian Academy of Sciences; [2] Northern Arctic Federal University, Arkhangelsk, Russia.[3]Laboratory for Ecology of Aquatic Communities and Invasions, A.N. Severtsov Institute of Problems of Ecology and Evolution, Russian Academy of Sciences, Moscow, Russia. [4]Department of Natural Resources and Rural Development, Norwegian Institute of Bioeconomy Research, Svanhovd, Svanvik, Norway. [5]Municipal Department 45 – Water Management, Vienna City Administration, Vienna, Austria. [6]Department of Invertebrate Zoology, Saint Petersburg State University, Saint Petersburg, Russia. [7]Department of Palaeontology, Geozentrum, University of Vienna, Vienna, Austria. [8]Department of Applied Ecology, Saint Petersburg State University, Saint Petersburg, Russia. [9]Section of Invertebrate Zoology, Göteborg Natural History Museum, Göteborg, Sweden. [10]Museum of History of Science and Technology, University of Latvia, Riga, Latvia. [11]Finnish Museum of Natural History, University of Helsinki, Helsinki, Finland. 12Laboratory of Macroecology and Biogeography of Invertebrates, Saint Petersburg State University, Saint Petersburg, Russia. [13]Laboratory of Evolutionary Biology of Development, N.K. Koltzov Institute of Developmental Biology of Russian Academy of Sciences, Moscow, Russia

Background

Many ecosystems are threatened because of climate warming, which affects the status of populations of individual species, their ecological functions and interspecific interactions.

The strongest impacts of warming water appear to be on cold-water ecosystems, such as oligotrophic streams and rivers.

Background

The rapid rise in water temperature in European lotic systems in recent decades has been confirmed. The studies reveal that among hydro-climatological variables, change in air temperature, which is a response to climate forcing, is the main driver of river temperature change. Unfortunately, the effects of climate change on oligotrophic rivers and their communities are investigated only at local and regional.

Background



Our study species is the freshwater pearl mussel

***Margaritifera margaritifera* (L., 1758)**

which is among the most critically endangered freshwater animals at the global scale. This species exclusively inhabits cold running waters with low mineralization and organic content and is unique because of its very high longevity (up to 280 years) and narrow host specialization.





Background

The distribution and abundance of *M. margaritifera* have drastically decreased throughout Europe over the last century, particularly within the southern part of the range and the majority of its populations has lacked successful reproduction for last 30–50 years.

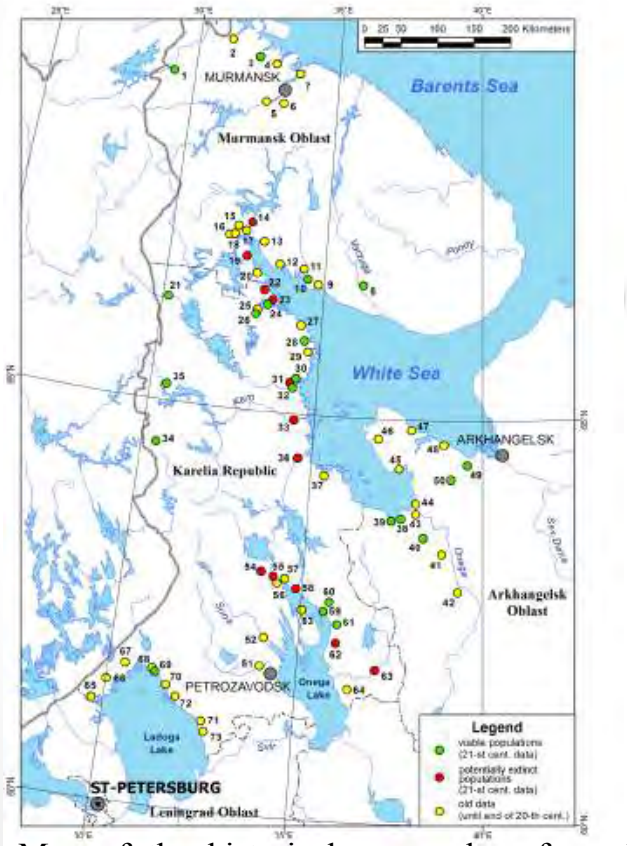


Fig. Map of the historical geography of pearl harvesting and current status of the freshwater pearl mussel (*M. margaritifera*) populations in Northwestern Russia
Makhrov et al., 2014 (*Hydrobiologia)*



Fig. Map of the study area. (•) Locations of the rediscovered populations: (1) Okhta, (2) Sestra, (3)Gladyshevka, (4) Roschinka, (5) Peypia, (6) Yanega, (7) Shotkusa, (8) Khorinka. (+) Locations of extinct populations. (*) River locations where no pearl mussels were detected.
Popov, Ostrivsky, 2014 (*Hydrobiologia)*

Background

The indirect effects associated with anthropogenic transformations, such as:

a) Habitat loss, fragmentation and degradation;

(b) Overexploitation and salmonid host overfishing;

(c) Pollution and eutrophication.

Background



Dam in Solsa River, Russia

Pearl industry in the territory of contemporary Arkhangelsk oblast.


A


B


C

Pearl mussel expedition in the Kazanka River under the supervision of I.V. Guttuev in July 1929: (a, b) - expedition members, (c) - pearl mussel fishing.









Girl headband and headpiece kokoshnik the XIX century - the beginning of XX century

Background

A number of populations in the streams flowing into Lake Imandra died out, and the Umba River population was heavily impaired by industrial pollution (Ziuganov et al., 1994).



Monchegorsk, Imandra Lake

However, little attention has been paid to global climate change as a possible factor in population decline.

The main goals of the present study:

(i) perform a series of regression models describing the influence of climatic variables on the shell convexity, age and status of freshwater pearl mussel populations at the continental scale;

(ii) produce a series of temperature dependent integrative models of climatically suitable areas for freshwater pearl mussels throughout Europe during past and future periods on the basis of morphometric, ecological and climatic data;

(iii) discuss the possible influence of climate warming on freshwater pearl mussel population decline during the last century.



Methods

Data sampling.

In this study, 3279 shells of *Margaritifera margaritifera* from 50 rivers and 6 countries across the freshwater pearl mussel range in Europe were used.

A total of **2985** shells from **49** recent populations were studied (1984–2013; n > 10 specimens in each sample).

Additionally, we used **294** shells from 13 historical samples (~1840–1940; n ≥ 5 specimens in each sample) found in the museum collections.



Methods

The museum collections used are as follows:

- IPEE - A.N. Severtsov Institute of Problems of Ecology and Evolution of the Russian Academy of Sciences, Moscow, Russia
- MNHN – Musèum National d'Histoire Naturelle, Paris, France
- NHMG – Göteborg Natural History Museum, Göteborg, Sweden
- RMBH – Russian Museum of Biodiversity Hotspots, Federal Center for Integrated Arctic Research of the Russian Academy of Sciences, Arkhangelsk, Russia
- SMNH – Swedish Museum of Natural History, Stockholm, Sweden
- ULMHST – Museum of History of Science and Technology, University of Latvia, Riga, Latvia
- ZIN – Zoological Institute of the Russian Academy of Sciences, St. Petersburg, Russiahttps://www.zin.ru/img/me

Methods

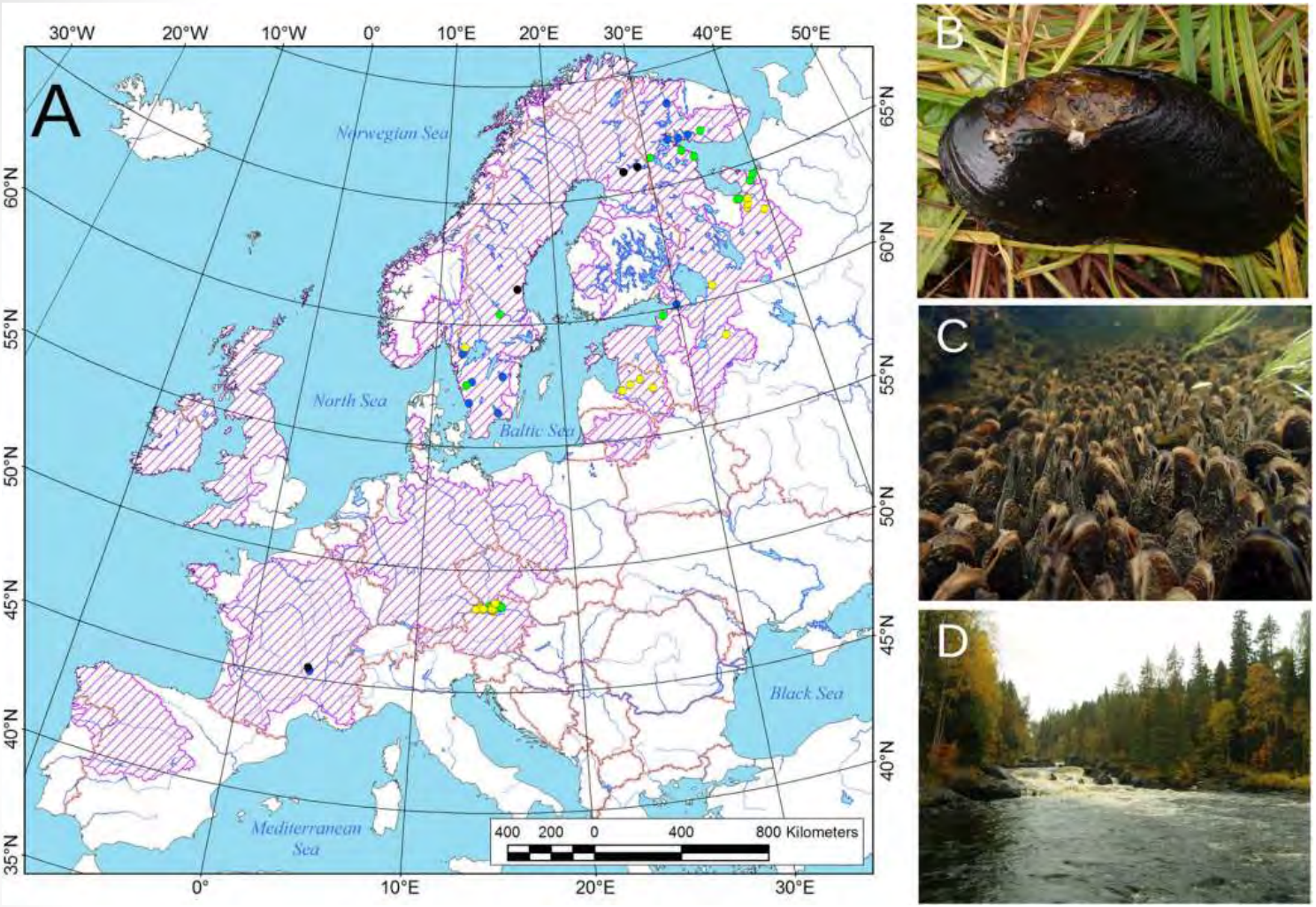


Figure 1. European distribution range of *Margaritifera margaritifera* with our sampling localities, adult mussels and their habitat. (**A**) Map of the distribution range of the freshwater pearl mussel in Europe and our sampling localities. **The pink hatching indicates the approximate distribution range of the species. Blue dots indicate historical samples (~1840–1940; *n* = 13); yellow dots indicate recent declining populations (1984–2013; *n* = 24); green dots indicate recent viable populations (1984–2013; *n* = 21); and black dots indicate recent populations with unknown status (1984–2013; *n* = 4).** Map was performed by using ESRI ArcGIS 10 software (www.esri. com/arcgis). The base of the map was created with Natural Earth Free Vector and Raster Map Data (www. naturalearthdata.com). (**B**) A mussel specimen. (**C**) Undisturbed mussel bed, Finland (photo: Panu Oulasvirta). (**D**) Habitat, NW Russia.

Methods

We measured three shell dimensions for each specimen using calipers (±0.1 mm): **the length (L), height (H)**, and **width (W)** of the shell, all taken at the maximal diameter.

To minimize morphological differences between populations resulting from the ontogenetic heterogeneity of their individuals, all mussels with shell lengths less than 5 cm were excluded from the compiled data set.













Methods

Supplementary Table 1. Summary of mean shell parameters, morphometric indices and maximum ages in *Margaritifera margaritifera* populations in the analyzed dat
set

Country	Drainage	River or stream	Locality	River size group*	Year of shell collecting	Period of shell collecting	Sample type**	Number of shells (N)	Coordinates (decimal degrees)		Altitude, m a.s.l.	Shell length (L), mm				Max. shell height (H), mm				Shell width (W), mm				Shell convexity index (SCI = W/L×100)				Elongated shell convexity index ($(L/L_A - W/L_A)^{1.5}$×100)				Max. age, years	Source of max. age assessment
									Latitude	Longitude		Mean	Min	Max	SD	Mean	Min	Max	SD	Mean	Min	Max	SD	Mean	Min	Max	SD	Mean	Min	Max	SD		
France	Adour Ocean	Lees River	Cauneres-en-Arbyre	Lowland	1973	Historical	MC (MNHN)	5	43.3319	-0.8469	934	96.7	87.0	104.2	6.3	43.4	42.0	44.7	2.2	23.9	23.0	26.4	1.0	24.48	24.04	25.00	0.40	31.76	30.69	32.80	0.80	50	50
Taiwan	Dongjiang River — Bohai Sea	Tianmaqu Stream	Tianmaqu 1 (old)	Lowland	1998	Historical	MC (LSAMNH)	15	25.2553	26.0505	120	50.7	35.3	104.5	21.0	35.1	25.1	52.4	6.4	27.5	20.0	34.5	3.5	70.81	53.86	91.42	7.85	13.85	11.49	16.06	1.75	50	50
Russia	Baltic Sea	Neste River	Neste Mouth (old)	Lowland	1993	Historical	MC (ZIN)	5	60.1491	28.9573	7	98.2	79.3	115.3	13.4	47.3	39.1	53.2	6.4	39.1	33.9	39.7	3.4	39.69	33.95	48.28	5.68	13.68	10.69	23.93	6.69	50	50
Russia	Kuzp River — White Sea	Chirvinka River	Chirvinka (old)	Lowland	1936	Historical	MC (ZIN)	12	66.1858	33.8897	78	92.4	83.9	107.8	8.4	45.5	35.3	57.6	5.7	48.8	38.6	57.6	4.1	50.73	34.09	92.16	3.80	53.48	38.93	86.54	4.80	50	50
Russia	Solza River — White Sea	Kolomka River	Kolomka (old)	Lowland	1970	Historical	MC (ZIN)	11	64.3623	38.6990	91	105.7	90.3	119.6	14.7	53.1	42.4	61.7	5.0	29.6	23.9	35.0	3.4	27.21	24.17	30.18	1.77	14.89	10.70	21.01	1.27	50	50
Russia	Umba River — White Sea	Lyuvenskaya River	Lyuvenskaya (old)	Lowland	1936	Historical	MC (ZIN)	48	66.6663	34.9564	89	77.6	55.3	102.1	9.8	37.3	24.3	45.9	3.9	23.0	16.0	27.1	1.9	27.06	24.24	30.74	1.22	22.93	17.68	27.97	1.76	50	50
Russia	White Sea	Pu'ja River	Pu'ja Bay (old)	Lowland	1960	Historical	MC (ZIN)	11	64.8207	34.5395	5	110.6	99.5	134.5	10.0	45.3	40.5	48.5	2.7	35.0	30.8	37.6	1.9	31.67	24.81	39.07	1.90	31.84	29.75	34.90	1.91	50	50
Russia	White Sea	Tkhamichikhinca River	Tkhamichikhinca (old)	Lowland	1936	Historical	MC (ZIN)	16	66.8659	32.4616	16	75.9	58.2	104.5	13.4	39.8	27.5	52.5	6.6	48.5	33.9	52.3	6.1	64.48	52.09	77.20	3.46	64.43	47.08	84.87	3.57	80	Red ring
Sweden	Baltic Sea	Bråbodsån Stream	West of Örebro	Lowland	1986	Historical	MC (SMNH)	37	59.1667	15.0057	161	111.1	90.1	137.3	7.6	50.1	42.4	55.7	3.1	29.6	23.9	35.3	2.7	26.94	19.04	39.90	2.42	23.37	17.94	34.62	2.46	50	50
Sweden	Gårdsjö River — North Sea	Rådasbrogen Stream	East of Bäcke church	Lowland	1989	Historical	MC (SMNH)	19	58.1993	12.0864	150	105.9	89.1	145.2	14.3	39.8	33.5	51.7	4.5	39.3	33.5	46.5	3.7	38.82	35.95	45.24	2.75	23.18	21.21	26.20	1.50	50	50
Sweden	Ivösjön Lake — Mörrum River — Baltic Sea	Bosarpsån Stream	East of Norra Vi Church	Lowland	1999	Historical	MC (SMNH)	0	55.6663	13.3960	175	105.7	76.3	130.9	16.7	38.5	33.6	46.7	4.5	29.2	23.4	32.9	2.2	27.69	26.06	30.12	1.66	23.66	21.75	26.02	0.69	50	50
Sweden	Simrån River — North Sea	Vidsträndsån Stream	Vidsträndsån 1	Lowland	1985	Historical	MC (SMNH)	30	56.3303	12.7875	35	85.9	65.5	107.1	10.5	34.9	29.0	43.0	3.3	32.9	25.5	38.1	3.0	38.05	31.89	29.67	3.96	34.84	19.03	50.61	3.57	50.3	50
Sweden	Verkan River — North Sea	Rönn-Åbyhov Stream	Rönnåsa	Lowland	1999	Historical	MC (SMNH)	0	57.6706	12.9416	160	80.1	51.3	103.2	14.1	30.5	16.0	38.4	4.0	24.7	15.2	30.9	4.1	31.64	23.15	38.61	3.42	29.99	19.73	33.98	4.25	50.4	50
Siberia	Danube River — Black Sea	Aufbach, Stream	Pionerskoe town/Lotzbach	Upland	1997	Recent	FM	48	48.4581	21.6387	600	103.1	90.4	119.6	10.1	39.6	33.6	48.0	4.1	30.4	19.0	37.9	3.4	38.92	27.42	50.79	3.35	34.75	19.75	57.61	3.51	95	Original
Siberia	Danube River — Black Sea	Tiverets Creek Stream	Divnoe town/Lotzbach	Upland	1997	Recent	FM	49	48.4488	21.8950	530	98.5	78.6	112.0	9.9	38.4	30.9	45.6	3.1	28.3	19.5	34.0	3.1	28.45	19.86	32.19	1.89	23.91	19.04	28.89	1.77	77	Original
Siberia	Danube River — Black Sea	Tekkatei Stream	Upper reaches of Rundbach	Upland	1997	Recent	FM	16	48.3776	24.4472	667	96.1	68.6	112.0	9.9	44.6	34.0	53.6	5.0	28.7	23.6	33.0	3.1	30.60	26.00	33.65	2.47	24.45	22.86	27.26	0.65	94	Original
Siberia	Danube River — Black Sea	Glubokiy Kamp Stream	Novosvit/Shumbach	Upland	1997	Recent	FM	47	48.3987	23.0161	600	95.1	58.6	115.0	12.6	43.0	29.0	52.6	5.6	36.6	17.6	52.4	5.8	36.27	22.95	51.43	3.64	23.42	10.00	36.61	3.37	94	Original
Siberia	Danube River — Black Sea	Shelkovskoe Stream	Shelkovskoe	Upland	1998	Recent	FM	35	48.5200	24.0004	470	109.5	82.0	133.0	9.8	39.5	42.0	58.0	3.9	39.0	16.0	51.6	5.3	28.85	24.07	32.87	1.95	23.06	20.85	25.98	1.20	52	Original
Siberia	Danube River — Black Sea	Kamp River	Lisnovskoe	Upland	1997	Recent	FM	71	48.5011	23.2179	501	97.6	70.0	123.0	12.6	43.5	27.0	54.0	3.0	33.6	16.0	52.0	8.3	34.48	23.08	49.86	3.42	22.27	10.58	34.79	3.06	94	Original
Siberia	Danube River — Black Sea	Kamyanka Stream	Upper reaches of Serebrianka/Lipki	Upland	1998	Recent	FM	22	48.3495	24.7952	589	80.0	58.6	100.0	11.5	33.1	20.0	44.0	5.3	30.7	16.0	39.0	3.5	38.42	27.12	51.61	3.39	34.79	23.06	47.73	4.32	45	Original
Siberia	Danube River — Black Sea	Krasne-Stolb Stream	Upper reaches of Dubrulia/	Upland	1997	Recent	FM	48	48.4229	24.1981	525	95.0	68.0	109.0	8.7	44.1	33.0	57.0	4.4	34.1	23.0	45.0	3.6	35.94	25.27	55.36	3.84	23.65	22.06	26.81	1.45	47	Original
Siberia	Danube River — Black Sea	Dzvinkhuk Stream	Gerling	Upland	1997	Recent	FM	36	48.4820	24.0844	481	79.1	59.4	97.0	9.2	39.7	28.0	46.0	3.8	34.3	27.0	39.0	2.5	38.79	28.46	44.72	3.35	24.01	22.25	27.35	1.09	60	Original
Siberia	Danube River — Black Sea	Ryzenbach Stream	Wolfsbrun	Upland	1998	Recent	FM	0	48.5166	23.9867	300	85.1	56.0	112.0	10.1	42.4	32.0	57.0	4.3	36.6	16.0	50.0	5.1	33.61	24.31	44.26	3.43	24.76	11.68	36.05	3.17	91	Original
Siberia	Danube River — Black Sea	Pilshibach Stream	Upper reaches of Ardzrill	Upland	1997	Recent	FM	36	48.4481	24.4238	500	105.1	87.0	126.0	8.6	49.4	43.0	58.0	4.7	43.8	27.0	58.0	4.8	46.66	35.00	56.47	3.35	32.02	23.81	38.66	3.46	85	Original
Siberia	Danube River — Black Sea	Pilshibach Stream	Upper reaches of Malynivtsi	Upland	1998	Recent	FM	35	48.4201	23.8658	500	108.1	82.0	133.0	9.0	49.9	40.0	57.0	3.9	30.9	18.0	45.0	5.2	28.82	23.69	35.29	2.59	24.83	20.45	27.79	1.75	98	Original
Siberia	Danube River — Black Sea	Pasechnaya Stream	Kl. Wolfsbrunch	Upland	1997	Recent	FM	46	48.7369	25.3303	708	86.4	60.0	97.0	6.8	38.6	36.0	43.0	1.6	23.7	16.0	36.0	3.6	27.35	21.65	31.33	1.62	21.35	16.79	26.64	1.34	61	Original
Siberia	Danube River — Black Sea	Pasechnaya Stream	Bagbotivka	Upland	1997	Recent	FM	33	48.5434	25.3928	450	89.9	79.0	108.0	7.6	33.0	24.0	51.0	4.9	19.7	16.0	32.0	3.3	18.43	15.94	25.15	1.75	15.42	13.92	16.51	1.52	61	Original
Siberia	Danube River — Black Sea	Pasechnaya Stream	Gnylitsa/Lipig	Upland	1997	Recent	FM	33	48.6986	25.1787	767	87.9	58.0	98.0	9.1	36.3	30.0	44.0	4.1	28.3	16.0	39.0	3.7	28.36	17.86	34.68	3.49	23.72	19.68	25.70	0.83	98	Original
Siberia	Danube River — Black Sea	Pasechnaya Stream	Watermill near Rapperschitsy	Upland	1997	Recent	FM	35	48.5397	25.2466	685	91.0	79.0	105.0	7.0	41.8	33.0	51.0	4.4	35.6	17.0	51.0	6.1	36.92	31.25	47.50	3.26	23.47	18.76	25.93	1.90	61	Original
Siberia	Danube River — Black Sea	Wolfsbrut River	Feldmühl	Upland	1998	Recent	FM	31	48.3981	24.0192	487	98.4	19.0	110.0	13.6	52.9	36.0	63.0	5.1	20.2	16.0	38.0	2.7	36.80	24.11	40.68	3.69	34.84	19.07	41.06	3.92	50	Original
Siberia	Danube River — Black Sea	Wolfsbrut River	Shubinskie	Upland	1997	Recent	FM	11	48.4366	24.5127	592	86.6	16.0	127.0	12.7	34.2	27.0	53.6	3.2	22.7	17.0	36.0	3.1	26.37	21.57	40.00	2.70	21.27	16.24	31.00	2.69	90	Original
Siberia	Danube River — Black Sea	Wolfsbrut River	Shubinskie	Upland	1997	Recent	FM	58	48.4180	24.6400	514	91.5	18.0	113.0	13.9	34.9	19.0	49.9	4.5	30.0	16.0	50.0	3.6	37.79	19.81	50.91	3.42	22.95	19.67	29.06	1.81	98	Original
Ukraine	Dniester River — Black Sea	Lomnytsi Stream	St. Mikuly	Upland	1997	Recent	FM	35	48.6940	24.8343	651	95.8	18.0	113.0	10.8	39.2	37.0	50.0	3.1	37.2	23.0	50.0	3.1	39.41	26.67	51.98	3.33	23.66	17.04	26.09	1.55	35	Original
Finland	Oulu River — Baltic Sea	Livojoki Stream	Livojoki 1	Lowland	1999	Recent	FM	32	65.5083	27.5368	85	108.7	95.5	117.5	5.5	47.5	32.0	53.0	4.1	35.1	30.0	37.0	3.5	29.07	26.60	33.02	1.77	13.90	10.74	17.50	1.50	50.2	50
Finland	Oulu River — White Sea	Iwojoki Stream	Iwojoki 1	Lowland	1999	Recent	FM	29	66.0349	26.4302	161	85.0	70.0	100.5	14.7	43.2	34.5	59.0	5.0	23.0	20.0	45.5	5.5	30.09	26.03	51.15	4.85	23.19	16.33	29.28	3.99	50.4	50
Finland	Lake River — Atlantic Ocean	Tornio River	Tornio	Upland	1994	Recent	MC (MNHN)	11	65.4513	23.7577	268	79.0	64.1	92.5	9.6	38.2	37.5	47.8	3.5	23.5	20.1	26.1	3.3	29.65	25.85	34.85	2.45	23.67	20.78	27.99	1.56	50.4	50
Latvia	Daugava River — Baltic Sea	Podzikas Stream	Podzikas 1	Lowland	2017	Recent	FM	35	56.9577	26.9997	97	110.9	86.5	139.0	10.5	53.0	40.0	68.0	4.3	31.0	24.0	39.0	3.4	28.63	20.01	36.00	3.21	13.75	10.99	29.01	3.69	50.4	50
Latvia	Daugava River — Baltic Sea	Tomsons Stream	Tomsons 1	Lowland	2017	Recent	FM	42	57.1951	26.0208	108	90.8	67.5	105.0	8.6	43.7	33.6	49.6	3.8	26.7	20.5	31.6	2.8	30.44	25.66	36.60	2.08	24.41	20.82	29.90	1.76	50.4	50
Latvia	Gauja River — Baltic Sea	Pelitupe Stream	Pelitupe 1	Lowland	2017	Recent	FM	37	57.1950	25.2201	151	108.4	85.0	133.5	9.4	50.0	34.0	61.5	3.9	32.0	27.0	38.5	3.3	34.82	27.75	38.57	2.35	24.88	21.35	30.97	1.67	50.4	50
Latvia	Gauja River — Baltic Sea	Rauna River	Rauna 1-2	Lowland	2009–2012	Recent	FM	167	57.1693	24.9726	26	89.3	64.0	130.0	13.6	40.3	29.0	64.5	6.3	29.6	17.0	49.0	4.5	36.80	22.89	50.61	3.66	24.08	14.73	28.90	3.48	50.4	50
Russia	Baltic Sea	Pyyjoki River	Pyyjoki 1	Lowland	2011	Recent	MC (SMNH)	111	59.7001	26.7059	5	108.5	79.0	134.0	13.3	38.4	34.5	41.5	3.6	30.1	20.5	40.5	4.9	28.17	17.28	33.05	3.08	17.54	10.05	27.99	3.74	50	Original
Russia	Neva River — Baltic Sea	Khoroshka River	Khoroshka 1	Lowland	2011–2012	Recent	MC (ZIN)	78	59.8530	31.2621	42	72.0	55.4	100.1	12.6	33.3	27.5	41.9	4.0	22.0	16.0	31.0	4.5	30.67	24.39	39.80	3.19	23.46	19.08	27.82	1.85	50	Original
Russia	Neva River — Baltic Sea	Sestroretsk River	Sestroretsk 1	Lowland	2011–2012	Recent	MC (ZIN)	41	60.1277	29.9781	47	107.0	79.0	135.7	11.7	46.7	34.5	60.4	4.5	37.6	29.0	47.0	3.1	34.78	26.75	42.00	3.78	23.49	16.51	27.60	1.79	50	Original

Methods

Morphometric analyses, population status assessment and general linear models (GLMs).

We calculated the basic morphometric index, namely the **shell convexity index**, SCI (W:L ratio ×100).

In addition, we computed the integrated shell convexity index, SCI_I:

$SCI_I = W/SA^{½} \times 100$, where SA is a sagittal area calculated using an ellipse formula ($\pi \times L \times H$).

However, the SCI_I was found to be a function of the traditional SCI (Pearson's $r = 0.96$, $n = 62$, $P < 0.001$) and was not used as a separate parameter.

Results

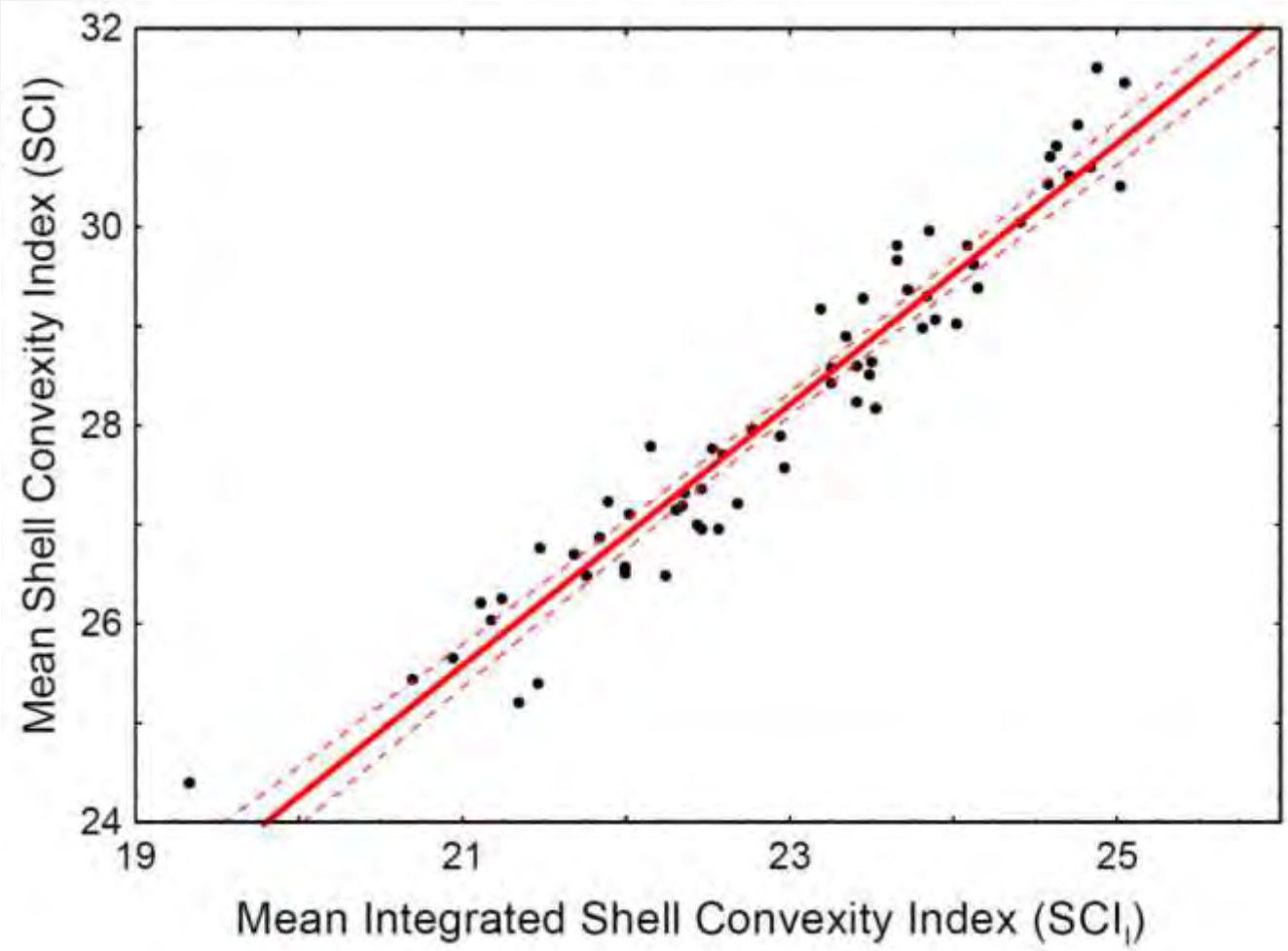


Figure 1. Mean shell convexity index (SCI) vs. mean integrated shell convexity index (SCII) scatterplot in *Margaritifera margaritifera* populations from across Europe (full data set, $n = 62$). The dashed lines are the 95% confidence bounds of the regression model.

Methods

- Additionally, we checked the assumption regarding the influence of sample size (number of mussels measured) on the index values using Spearman's correlation test. We determined that the variability of both the mean SCI and SCI_I values are not correlated with sample size (Spearman's $r = 0.17$, $n = 62$, $P > 0.05$).

Methods

The status of recent populations was estimated as follows (Geist 2011):

(i) viable (functional) populations with high mussel density, and high or moderate recruitment, and

(ii) declining (non-functional) populations with moderate or low mussel density, and low or no recruitment.

Supplementary Table 2. Assessment of the status of European *Margaritifera margaritifera* populations in the analyzed data set (recent samples)

Country	Drainage	River or stream	Locality	River site group*	Year of shell collecting	Population status**	Time period of the population status assessment	References
Austria	Danube River => Black Sea	Aubach Stream	Downstream of Leithen	Upland	1992	declining	1992-2002	Refs. 26, 46
Austria	Danube River => Black Sea	Daglesbach Stream	Downstream of Lembach	Upland	1992	declining	1992-2002	Refs. 46, 47
Austria	Danube River => Black Sea	Feldaist Stream	Upstream of Rainbach	Upland	1992	viable	1992-2002	Refs. 26, 46
Austria	Danube River => Black Sea	Großer Kamp Stream	Neustift/Hausbach	Upland	1992	viable	1992-2002	Refs. 26, 46, 47
Austria	Danube River => Black Sea	Harbe Aist River	Neuhof	Upland	1992	declining	1992-2002	Refs. 26, 46, 47
Austria	Danube River => Black Sea	Kamp River	Utissenbach	Upland	1992	viable	1992-2002	Refs. 26, 46, 47
Austria	Danube River => Black Sea	Kleine Naarn Stream	Upstream of Steinbruckmühle	Upland	1992	declining	1992-2002	Refs. 26, 46
Austria	Danube River => Black Sea	Kleine Rodl Stream	Upstream of Eidendorf	Upland	1992	declining	1992-2002	Refs. 26, 46
Austria	Danube River => Black Sea	Pesenbach Stream	Gerling	Upland	1992	declining	1992-2002	Refs. 26, 46
Austria	Danube River => Black Sea	Pesenbach Stream	Waldhofer	Upland	1992	declining	1992-2002	Refs. 26, 46
Austria	Danube River => Black Sea	Pfudabach Stream	Upstream of Angsüß	Upland	1992	declining	1992-2002	Refs. 26, 46
Austria	Danube River => Black Sea	Pfudabach Stream	Upstream of Mitterndorf	Upland	1992	declining	1992-2002	Refs. 26, 46
Austria	Danube River => Black Sea	Purzelkamp Stream	Kl. Weißenbach	Upland	1992	viable	1992-2002	Refs. 26, 46
Austria	Danube River => Black Sea	Purzelkamp Stream	Rappoltschlag	Upland	1992	viable	1992-2002	Refs. 26, 46
Austria	Danube River => Black Sea	Purzelkamp Stream	Grafenschlag	Upland	1992	viable	1992-2002	Refs. 26, 46
Austria	Danube River => Black Sea	Purzelkamp Stream	Watermill near Rappoltschlag	Upland	1992	viable	1992-2002	Refs. 26, 46
Austria	Danube River => Black Sea	Waldaist River	Feiblmühl	Upland	1992	declining	1992-2002	Refs. 26, 46-49
Austria	Danube River => Black Sea	Waldaist River	Haidmühle	Upland	1992	declining	1992-2007	Refs. 26, 46-49
Austria	Danube River => Black Sea	Waldaist River	Riedelhammer	Upland	1992	declining	1992-2007	Refs. 26, 46-49
Austria	Elbe River => North Sea	Lainsitz Stream	St. Martin	Upland	1992	declining	1992-2002	Refs. 26, 46, 47
Finland	Iijoki River => Baltic Sea	Livojoki Stream	Livojoki 1	Upland	1989	N/A	N/A	N/A

Methods

- To estimate the relationship between **the growth constant (K)** and mean summer temperature, shell samples from 9 rivers (Keret', Kozha, Maloshuika, Mutkajoki, Nimen'ga, Peypia, Solza, Somba, and Yud'ma) were investigated.
- Five specimens were used from each sample (n = 45 in total). For all samples, at least 16 annual rings for each shell were measured. The growth constants were calculated using a data approximation based on the **recursive form of the Bertalanffy equation, i.e., the Ford-Walford equation**. The maximum age of individuals in a sample was calculated using a shell with the maximum length.
- Additionally, we incorporated **a sclera-chronological approach** by counting the annual rings in a thin transverse section of a valve. In some cases, a logarithmic equation describing the trend line on the annual growth length vs. age plot was also applied.

Methods

- To test the hypothesis of climate-induced morphometric differences between *M. margaritifera* populations the general linear models (**GLMs**) were used.
- We used shell width plotted against shell length as a covariate and population status as a factor with two levels.
- Additionally, we estimated differences between recent and historical samples using shell width plotted against shell length as a covariate and period of shell collecting as a factor with two levels.
- To test the assumption that latitude has different effects on the shell convexity at historical and recent time intervals, we applied a separate-slopes modeling approach using the mean **SCI** as a dependent variable, latitude as a continuous predictor, and two-level time interval as a categorical predictor.
- Correlation of morphometric parameters with climatic and geographic variables was calculated using Pearson's and Spearman's coefficients depending on sample size, type of variables and normality test results.

Modeling of freshwater pearl mussel response to climate change at the population level.

Methods

Monthly mean air temperatures were obtained from the CRU TS v. 3.23 climate database (Climatic Research Unit, University of East Anglia) as gridded variables (0.5° resolution), which were based on weather station records during the period from 1 January 1901 to 31 December 2014.



Methods

For each location of the samples, we calculated the mean summer temperature (MST) values for the 10-, 20-, 30-, 40- and 50-year periods before the year of each sample collection (number of available samples varied depending on the period of averaging from 49 to 55) in accordance with the slow growth rate and large longevity of the freshwater pearl mussels.

These parameters were estimated as possible predictors for the mean SCI values in pearl mussel populations using a simple linear regression model algorithm of STATISTICA 10 (Stat Soft Inc., USA).



Methods

Modeling of spatial distribution of climatically suitable areas of freshwater pearl mussel populations at the continental scale.

Methods

The general range model of *M. margaritifera* was processed using published mapping data, which was transformed to a gridded digital map (0.5 × 0.5°) using ESRI ArcGIS 10.

Further, we simulated a spatial distribution of climatically suitable areas for *M. margaritifera* populations across Europe based on this digital range model, in each grid cell of which a mean SCI value was calculated for each 20-year period, i.e., 1901–1920 and 1991–2010.



Methods

Using the spatial models outlined above, climatically suitable areas were mapped based on the estimated threshold SCI values in viable and declining populations. These threshold values for the SCI interval in declining populations were as follows:

$$A1 = A2 + 1.96 \times \text{s.e.m.} > A2 \geq A3 = (A2 + A4)/2;\ A4 < A3.$$

A1 represents the estimated 95% upper confidence boundary of the mean SCI in declining populations; A2 represents the mean SCI in declining populations; A3 represents a threshold SCI value between viable and declining populations;

A4 represents the mean SCI in viable populations; s.e.m. represents the standard error of the mean.



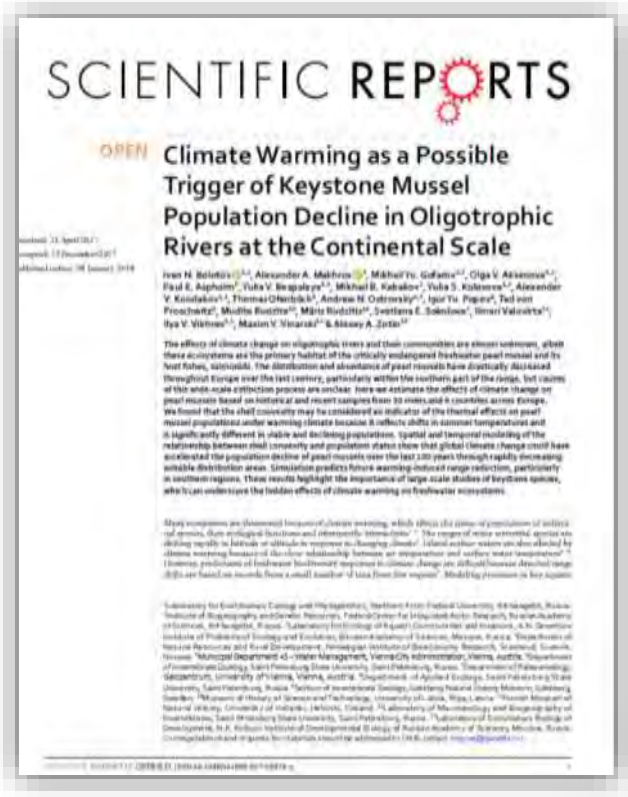
Results

Shell convexity changes in historical and recent *M. margaritifera* populations.

Results

Here we report the results of tests of the climate change effect on freshwater pearl mussel populations based on extensive morphological data sets obtained from 50 rivers and 6 countries across Europe: Austria, Latvia, Finland, France, Russia and Sweden.





SCIENTIFIC REPORTS

OPEN

Climate Warming as a Possible Trigger of Keystone Mussel Population Decline in Oligotrophic Rivers at the Continental Scale

Bolotov et al., 2018

SCI in historical pearl mussel samples from lowland rivers does not reveal a significant latitudinal trend. SCI in recent samples from lowland rivers increases from high to low latitudes.

The mean SCI in recent samples from mountain rivers at the regional scale (Austria) increases from high to low altitudes .

The mean SCI in recent samples from mountain rivers at the regional scale (Austria) increases from high to low altitudes .

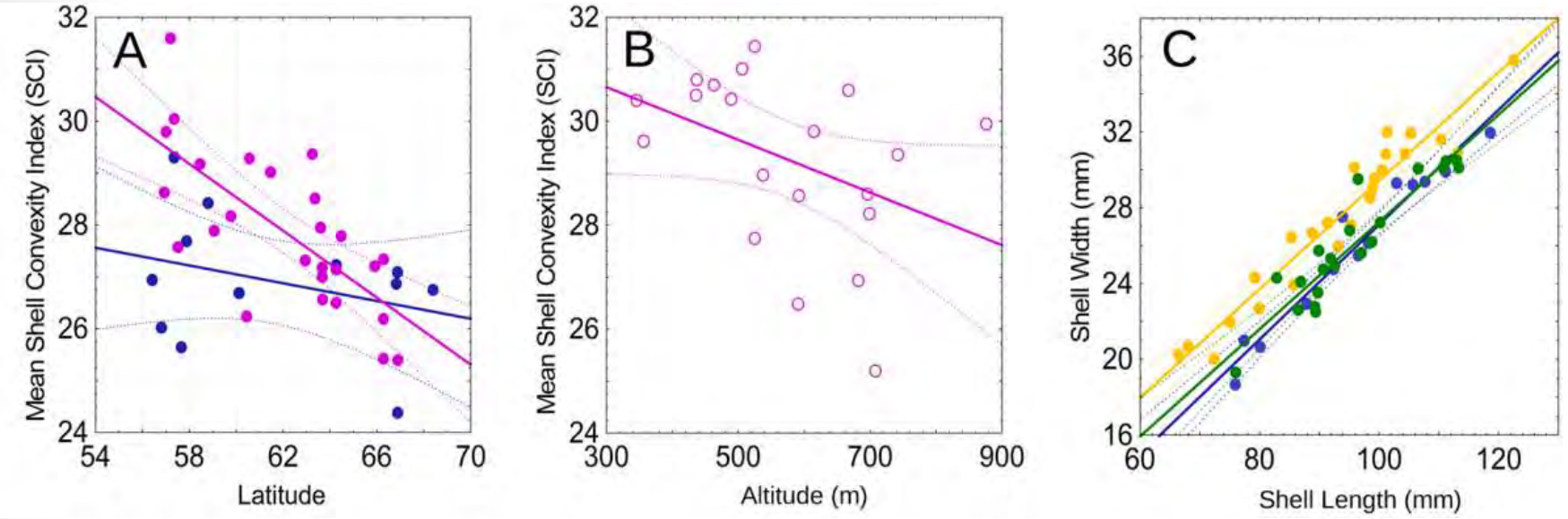


Figure 2. Variability of the relative shell convexity (SCI) and maximum age of *Margaritifera margaritifera* populations. The dashed lines are the 95% confidence bounds of the regression models. **(A)** Latitude vs. mean SCI scatterplot in populations from lowland rivers across Europe (<200 m altitude). Each point represents the mean value in a population; red points are recent lowland populations (1984–2013, n = 25, significant latitudinal trend: Spearman's rank correlation, P = 0.000001), and blue points are historical lowland populations (~1840–1940, n = 12, no significant latitudinal trend: Spearman's rank correlation, P = 0.53). **(B)** Altitude vs. mean SCI scatterplot in recent populations from mountainous rivers in Austria (>300 m altitude). Each point represents the mean value in a population (1992, n = 20, significant altitudinal trend: Spearman's rank correlation, P = 0.02). **(C)** Scatterplot of population shell length vs. shell width. Each point represents the mean value in a population; green points are recent viable populations (1984–2013, n = 21), yellow points are recent declining populations (1984–2013, n = 24), and blue points are historical populations (~1840–1940, n = 13).

Table 1. Results of general linear models (GLMs) of shell width in recent (1984–2013) and historical (~1840–1940) populations of *Margaritifera margaritifera*. Regression models were simplified to the minimal adequate models

Response variable	Source	Selected population groups: (i) recent viable and (ii) declining ($R^2 = 0.91$)				Selected population groups: (i) historical and (ii) recent viable ($R^2 = 0.91$)				Selected population groups: (i) historical and (ii) recent declining ($R^2 = 0.94$)			
		SS	*d.f.*	*F*	*P*	*SS*	*d.f.*	*F*	*P*	*SS*	*d.f.*	*F*	*P*
shell width	Intercept	—	—	—	n.s.	—	—	—	n.s.	—	—	—	n.s.
	length	32555.5	1	24740.6	<0.001	23308.6	1	18437.7	<0.001	24573.8	1	21576.3	<0.001
	Population group	51.9	1	39.4	<0.001	—	—	—	n.s.	47.6	1	41.8	<0.001
	Length × Population group	—	—	—	n.s.	—	—	—	n.s.	—	—	—	n.s.
	Error	56.6	43			41.7	33			39.9	35		

Results of general linear models (GLMs) revealed that in recent populations the relative shell width is significantly influenced by the population status independently of shell size; i.e., the mean SCI in recent declining populations differs from that for recent viable populations (Table 1).

Furthermore, based on GLMs, the relative shell width does not differ between recent viable populations and historical samples, but differs significantly between recent declining populations and historical samples (Table 1).

The impacts of climate change on the shell convexity in *M. margaritifera* populations.

We discovered that the mean SCI values in *M. margaritifera* samples are directly associated with mean air summer temperature (Fig. 2D; linear regression of the mean SCI versus mean summer temperature during the 20-year period before shell collecting (MST_{20}):

$$SCI = 18.207 + (0.666 \times MST_{20}); \text{ Pearson } r = 0.76, F1,47 = 64.2, P < 0.00001. \quad (1)$$

Additionally, there is a highly negative correlation between the mean SCI and the maximum age in populations (Fig. 2E; linear regression of the maximum age versus mean SCI:

$$A_{max} = 632.846 - (19.122 \times SCI); \text{ Pearson } r = -0.80, F1,28 = 48.7, P < 0.00001. \quad (2)$$

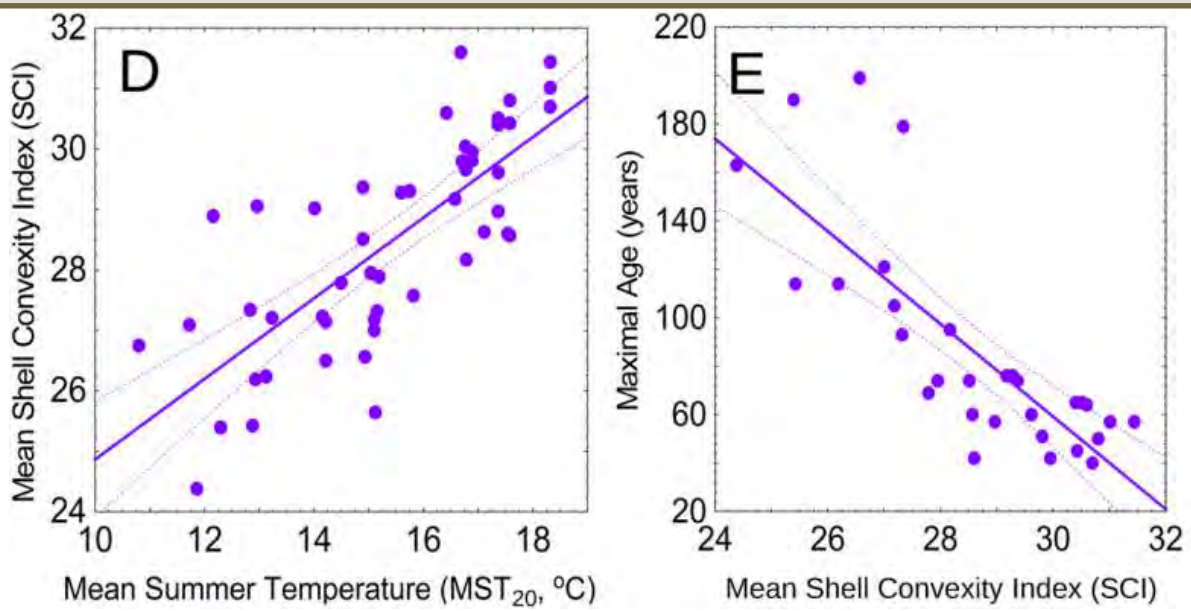


Figure 2. Variability of the relative shell convexity (SCI) and maximum age of *Margaritifera margaritifera* populations. (D) Scatterplot of mean summer temperature (MST20, 20-year mean before sampling) vs. mean SCI (equation 1). (E) Scatterplot of mean SCI vs. maximum age (equation 2). Each point represents the mean value in a population (n = 49).

Modeling of suitable areas for *M. margaritifera* under climate changes.

Results

Spatial modeling revealed that suitable areas for M. margaritifera were widely present in Central and Southern Europe during the cold period of 1901–1920. In contrast, these areas have been drastically reduced after climate warming during the period of 1991–2010. The spatial models of climatically suitable areas during the period of 2061–2080 under low, moderate and extreme climate change scenarios (Fig. 3C–F) predict almost complete disappearance of freshwater pearl mussels across Central and Southern Europe.

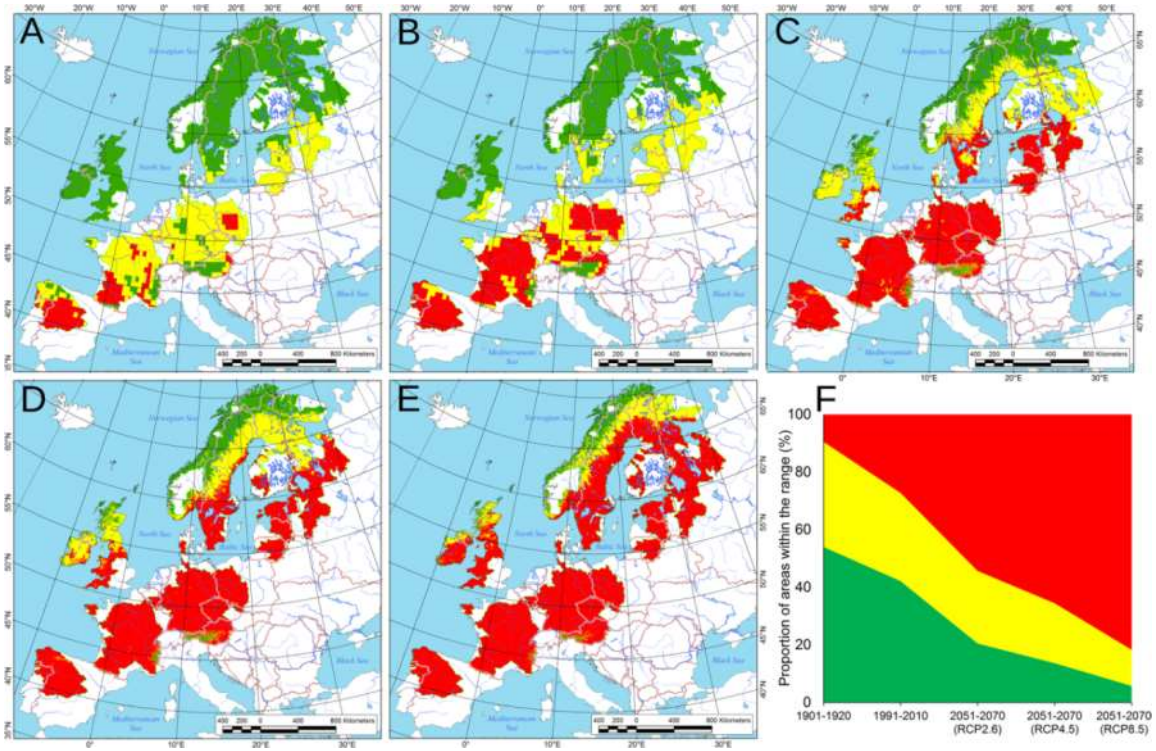


Figure 3. Spatial models of climatically suitable areas for freshwater pearl mussels across Europe in the past and future. Legend: green – suitable thermal conditions, viable populations; yellow – possible negative thermal effects, declining populations; red – most probably unsuitable areas. (**A**) Climatically suitable areas during the cold period from 1901–1920. (**B**) Climatically suitable areas during the warm period from 1991–2010. (**C**–**E**) Climatically suitable areas during the period from 2061–2080 under future climate change scenarios, low RCP 2.6 (**C**), moderate RCP 4.5 (**D**), and extreme RCP 8.5 (**E**). (**F**) Shift in climatically suitable areas based on spatial modeling.

Results

Reconstruction of long-term changes in the mean SCI in freshwater pearl mussel populations under climate fluctuations in the last 100 years (1901–2010) revealed the lowest index values at the beginning of the 20th century and the maximum during the warm period of 1991–2010. Correspondingly, reconstruction of maximum age changes indicated a significant decline in longevity during this time interval, particularly in recently declining populations.

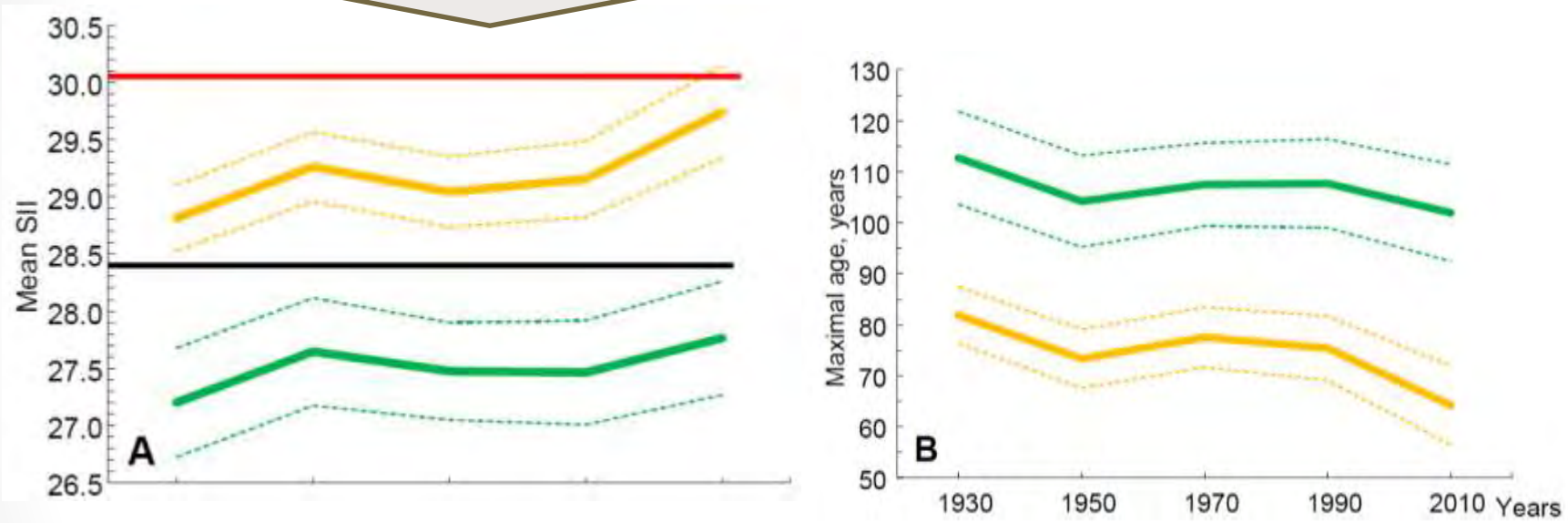


Figure 4. Models of the mean shell convexity index (SCI) and maximum age of freshwater pearl mussels across Europe in the past using MST20 data obtained from CRU TS v. 3.23 climate database (Climatic Research Unit, University of East Anglia). (**A**) Long-term changes in the mean SCI. The **green line indicates recent viable populations** (n = 15); **the yellow line indicates recent declining populations** (n = 24). The red line indicates the 95% upper threshold SCI value corresponding to the expected upper limit of thermal stress on the population level. The black line indicates the mean SCI threshold value between viable and declining populations (n = 45). (**B**) Long-term changes in the maximum age. The age values were calculated using equation 2. The **green line indicates recent viable populations** (n = 15); **the yellow line indicates recent declining populations** (n = 24).

The mean SCI in freshwater pearl mussel populations as an indicator of climate changes.

In general, the SCI reflects the temperature control of allometric growth that is expressed by shell convexity increasing with temperature via increased width of annual growth increments of the shell (Spearman's rank correlation between mean growth coefficient (K) and SCI: $r_s = 0.68$, $n = 9$, $P = 0.042$).

Our analysis showed that SCI may be considered as a possible indicator of the thermal effects on *M. margaritifera* populations under warming climate conditions because it directly reflects shifts in mean summer temperatures and is significantly different in viable and declining populations.

The effect of higher temperature on populations manifests itself in increased growth and metabolic rates, reduced longevity of adult mussels, high mortality of juveniles and restricted larval development.



Possible warming-driven decline of freshwater pearl mussels throughout Europe.

- the global climate change, may increase multiple negative effects from local and regional anthropogenic transformation of freshwater ecosystem.
- we suggest that cold climate periods contribute to optimal abiotic conditions for *M. margaritifera* as a keystone species and likely for oligotrophic river ecosystems as a whole
- the impact of which appears to be more significant in southern regions, this example of possible warming-driven species decline revealed that climate changes may have hidden effects on populations of individual species and on freshwater ecosystems
- our findings highlight the role of high-altitude rivers as local but important refugia for cold-adapted freshwater species such as *M. margaritifera* under future climate warming scenarios
- we revealed a new easy-to-obtain and low cost indicator of population status in freshwater pearl mussels (SCI) that may potentially be used for ecological monitoring of the populations of other threatened freshwater mussel species.

Conclusions

(1) Climate changes may trigger hidden extinction processes in freshwater animals such as freshwater pearl mussels in oligotrophic rivers and streams at the continental scale.

(2) The mean shell convexity in freshwater pearl mussel populations reflects shifts in summer temperatures and is significantly different in viable and declining populations. This parameter may be considered an easy-to-obtain and low-cost indicator of population-level thermal effects in freshwater pearl mussels under warming climate.

(3) The significant latitudinal trend in shell convexity of freshwater pearl mussel populations throughout Europe results from the recent warm climatic episode and was lacking in historical samples collected in 1840-1940. Spatial and temporal modeling of the relationship between shell convexity and population status show that global climate change could have accelerated the population decline of freshwater pearl mussels over the last 100 years through rapidly decreasing suitable distribution areas. Simulation predicts future warming-induced range reduction, particularly in southern regions.

(4) In southern areas, high-altitude rivers and streams will represent local but important refugia for cold-adapted species such as freshwater pearl mussel under future climate warming scenarios.

o



- **The next step** to estimate the global response of freshwater pearl mussels on climate warming based on an expanded dataset.

- We plan to calculate a series of regression models describing the influence of climatic variables on the shell convexity, age and status of freshwater pearl mussel populations in North America, Europe, and Asia. Based on the results of regression modeling, we will produce spatial models of climatically suitable areas for freshwater pearl mussels during past and future periods.

- Contact persons:

- *Ivan Bolotov* <inepras@yandex.ru>
- *Yulia Bespalaya* <*jbespalaja@yandex.ru*>

- Principal taxa:
- *M. margaritifera* - North America & Europe
- *M. falcata* - North America
- *M. dahurica* – Russian Far East
- *M. middendorffi* - Kamchatka to Japan
- *M. laevis* - Sakhalin to Japan
- Additional taxa:
- *M. auricularia* - Europe (+subfossil shells)
- *M. laosensis* - SE Asia (+subfossil shells)
- *M. monodonta* – North America



Acknowledgement

- The authors express their gratitude to all colleagues for their valuable assistance with the collecting and processing of material. The study has been supported by the program of the Presidium Ural Branch of RAS (no. 0409-2018-0148) and Russian Foundation for Basic Research (nos. 17-45-290066, 18-44-292001 p_mk and 17-44-290016).












YAKE




Thank you for your attention !